System Distortion Model for the Cross-Validation of Millimeter-Wave Channel Sounders

David G. Michelson[1], Camillo Gentile[2], Andreas F. Molisch[3], Jack Chuang[2], Anuraag Bodi[2], Anmol Bhardwaj[1], Ozgur Ozdemir[4], Wahab Ali Gulzar Khawaja[4], Ismail Guvenc[4], Zihang Cheng[3], Thomas Choi[3], Robert Müller[5]

[1] Dept. of Electrical & Computer Engineering, University of British Columbia, Vancouver, BC, Canada, *davem@ece.ubc.ca*
[2] Wireless Networks Division, National Institute of Standards and Technology, Gaithersburg, MD, USA
[3] Ming Hsieh Dept. of Electrical Engineering, University of Southern California, Los Angeles, CA, USA
[4] Dept. of Electrical & Computer Engineering, North Carolina State University, Raleigh, NC, USA
[5] Dept. of Electronic Measurements and Signal Processing Group, Technische Universität Ilmenau, Ilmenau, Germany

Abstract — **Because millimeter-wave directional channel measurements are time-consuming and expensive to collect, there is considerable interest in combining measurement data obtained with different channel sounders in order to yield more comprehensive datasets. The simplest way to verify that the results obtained with these different instruments in a given environment are comparable would be to transport the channel sounders to that environment, collect and process measurement data, and then compare the results. Because this is rarely feasible, we propose an alternative method that is much more practical. It involves: 1) Generating an ideal three-dimensional channel impulse response that corresponds to a scenario of interest, 2) Degrading the ideal response by applying a distortion model that capture the factors that limit the spatio-temporal resolution and dynamic range of each channel sounder, and 3) Applying the multipath component (MPC) extraction techniques used by the channel sounder to the distorted response. After the last step, one will observe: a) correctly estimated, b) incorrectly estimated, c) missing, and d) spurious MPCs. Discrepancies between the ideal and distorted responses will be readily apparent and the performance of the channel sounders can be easily compared in a given environment. The effort required to fully characterize the three-dimensional patterns of the transmitting and receiving antennas is considerable and further work is required to determine the corresponding accuracy requirements.**

***Index Terms*—Antenna, measurement, propagation.**

I. Introduction

Interest in directional channels was originally motivated by the development of smart antennas and multiple-input multiple-output antenna systems in the 1990's. Significant early contributions were made under the COST 259 project [1]. Until the mid-2000's, most efforts focused on bands below 6 GHz [2]. Current interest is strongly linked to recent efforts to develop mmWave (millimeter-wave) wireless technology for Wi-Fi and 5G wireless systems [3]. Because mmWave directional channel measurements are time-consuming and expensive to collect, there is considerable interest in comparing and possibly combining measurement data obtained with different channel sounders in order to yield more comprehensive datasets.

A variety of approaches and instrument configurations are currently used for mmWave channel sounding. Antennas may be steerable horns, virtual arrays, switched arrays or phased arrays. Probing signals may be swept frequency, multi-carrier or spread spectrum signals. After initial processing, MPCs may be extracted from received signals using algorithms such as SAGE, MUSIC, RiMAX, and CLEAN [4],[5],[6]. Before combining measurement data or intermediate results obtained with different channel sounders, it is essential to verify that the results returned by these different instruments are comparable. While the simplest approach would be to transport the channel sounders in question to a common environment, collect and process measurement data and compare the results, this is rarely practical.

The NIST-led 5G Millimeter-Wave Channel Model Alliance has brought together a large number of research labs from around the world to collaborate on mmWave channel measurement and modelling. A sub-group within the Alliance's working group on measurement techniques, including researchers from NIST, the University of British Columbia, the University of Southern California, North Carolina State University and the Technical University of Ilmenau, has taken up the challenge of devising a practical methodology for comparing the quality and resolution of measurements obtained using different channel sounders.

This work introduces and demonstrates a practical approach to comparing the performance of different channel sounders. The proposed methodology involves: 1) Generating an ideal three-dimensional channel impulse response that corresponds to a scenario of interest, 2) Distorting the ideal response by applying system model that captures the factors that determine the spatio-temporal resolution and dynamic range of each channel sounder, 3) Applying the multipath component (MPC) extraction techniques used by the channel sounder to the distorted response. Differences between the ideal and distorted three-dimensional channel impulse responses will be readily apparent

The remainder of this paper is organized as follows: In Section II, the proposed methodology is presented In Section III, the channel sounders used by the members of the subgroup and against which the procedure has been demonstrated are described and typical measurement and simulation results are presented. In Section IV, the outcomes of the work to date and issues to be addressed going forward are summarized.

II. Methodology

The proposed approach involves three steps. First, a space with dimensions comparable to the environment of interest and transmitting and receiving antenna locations corresponding to use cases of interest are defined. The ideal three-dimensional channel impulse response is then predicted using ray-tracing. Second, this ideal response is distorted by applying a system model that accounts for the limited spatio-temporal resolution and dynamic range of the channel sounder. These include the three-dimensional patterns of the transmitting and receiving antennas, the impulse response of the measurement system, and the system link budget including the system noise floor. Third, the MPC extraction technique used in conjunction with the channel sounder is applied to the distorted response to yield a final result. Discrepancies between the ideal and distorted responses will be readily apparent and the performance of the channel sounders can thus be compared.

A. Simulated Measurement Scenarios

The set of ideal channel responses provided by NIST was generated from the Quasi-Deterministic model for ten transmitter-receiver locations in a lecture room [7]. The map-based model uses the method of images to ray-trace the direct path and specular reflections (diffraction is neglected in light of its relative weakness at mmWave frequencies) given the geometry of the environment See Fig. 1. The ceiling, ground, and walls had different reflection losses characterized through measurement. A cluster of diffuse reflections (not shown) originating from surface roughness is associated with each specular reflection, multiplying the 21 specular reflections to nearly 500 combined. The cluster properties, such as angular spread (~3º) and the relative strength of the diffuse reflections with respect to the specular reflections (~6 dB), were also characterized through measurement. For the n^{th} ray, the polarization-dependent complex amplitude (a_n), delay (τ_n), and the Angle of Departure (AoD) ($\boldsymbol{\theta}_n^T = [\theta_n^{T,A}\ \theta_n^{T,E}]$) and Angle of Arrival (AoA) $\boldsymbol{\theta}_n^T = [\theta_n^{T,A}\ \theta_n^{T,E}]$) in both azimuth ($A$) and elevation ($E$) were outputted.

B. Array System Model

The channel impulse response measured by a channel sounder will be distorted compared to the ideal raytracing response due to the finite spatio-temporal resolution and sensitivity of the instrument. The effect will be to blur the rays, make it difficult to resolve rays that are closely spaced in angle or delay, and miss weaker rays. The instruments are operated in the linear regions of their components so non-linear distortions are not considered.

Consider a transmitting array centered at $\boldsymbol{x}^{T_0}$ and a receiving array centered at $\boldsymbol{x}^{R_0}$. When accounting for the individual contributions of the N rays, the channel response between the array centers is expressed as

$$y(\tau, \boldsymbol{x}^{T_0}, \boldsymbol{x}^{R_0}) = \sum_{n=1}^{N} a_n \cdot s(\tau - \tau_n) \cdot e^{j2\pi f_c(-\tau_n)},$$

where $s(\tau)$ is the band-limited transmitted signal (at baseband) and f_c is the center frequency.

A generic model for the array geometries is shown in Fig. 2, where $\boldsymbol{x}^{T_i}$ and $\boldsymbol{x}^{R_j}$ are the positions of the i^{th} transmitting and j^{th} receiving array element and $G^{T_i}(\boldsymbol{\theta}^{T_i})$ and $G^{R_j}(\boldsymbol{\theta}^{R_j})$ are their antenna patterns. It follows that the delay at $\boldsymbol{x}^{T_i}$ with respect to $\boldsymbol{x}^{T_0}$ is given by

$$\tau_n^{T_i} = \frac{u(\boldsymbol{\theta}_n^T) \cdot (\boldsymbol{x}^{T_0} - \boldsymbol{x}^{T_i})}{c}$$

and the delay at $\boldsymbol{x}^{R_i}$ with respect to $\boldsymbol{x}^{R_0}$ is given by

$$\tau_n^{R_j} = \frac{u(\boldsymbol{\theta}_n^R) \cdot (\boldsymbol{x}^{R_0} - \boldsymbol{x}^{R_j})}{c},$$

where the unit angle vector is given by

$$u(\boldsymbol{\theta}) = \begin{bmatrix} cos(\theta^A) \cdot sin\,(\theta^E) \\ sin(\theta^A) \cdot sin(\theta^E) \\ cos(\theta^E) \end{bmatrix}.$$

Finally, the distorted response between any two array elements is given by

$$\begin{aligned} y_w&\left(\tau, \boldsymbol{x}^{T_i}, \boldsymbol{x}^{R_j}, \boldsymbol{\theta}^{T_i}, \boldsymbol{\theta}^{R_j}\right) \\ &= \sum_{n=1}^{N} a_n\, G^{T_i}(\boldsymbol{\theta}_n^T - \boldsymbol{\theta}^{T_i}) \\ &\cdot G^{R_j}\left(\boldsymbol{\theta}_n^R - \boldsymbol{\theta}^{R_j}\right) \cdot s\left(\tau - \tau_n - \tau_n^{T_i} - \tau_n^{R_j}\right) \\ &\cdot e^{j\left[2\pi f_c\left(-\tau_n - \tau_n^{T_i} - \tau_n^{R_j}\right) + w_\phi(t)\right]} + w(t) \end{aligned}$$

where $w(t)$ and $w_\phi(t)$ are the thermal and phase noise components, respectively.

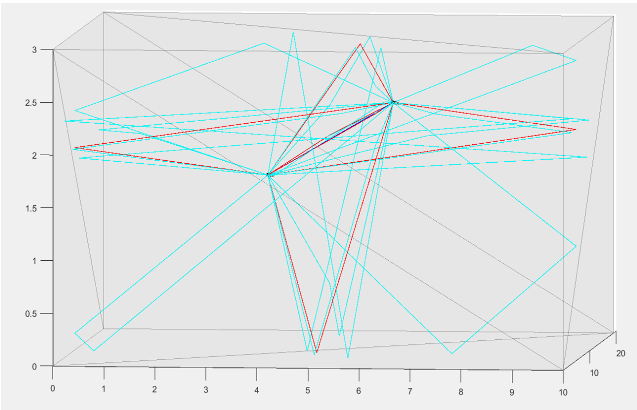

Fig. 1. An ideal three-dimensional channel impulse response within a 3 m ×10 m × 20 m box with transmitting and receiving antennas placed as shown as determined by ray-tracing. Besides the direct path (blue), there are six first-order reflections (red), and 15 second-order reflections (cyan).

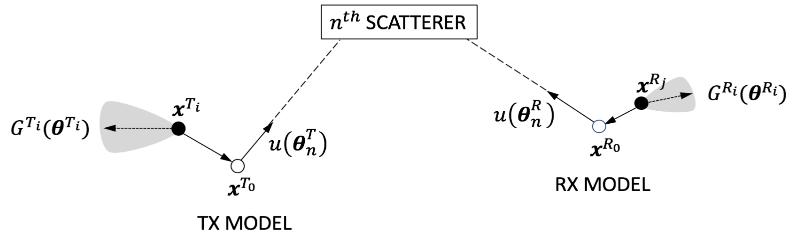

Fig. 2. Geometry of the array system model.

C. Application of the System Model

The ideal three-dimensional channel impulse response is distorted by applying the appropriate array system model described above to yield a distorted channel response, $y_w(t, \boldsymbol{x}^{T_i}, \boldsymbol{x}^{R_j}, \boldsymbol{\theta}^{T_i}, \boldsymbol{\theta}^{R_j})$. This response is then processed using the same ray-extraction algorithm used by the channel sounder on actual measured data, *e.g.,* SAGE, RiMAX, MUSIC, CLEAN, etc., to yield the estimated ray parameters, $\hat{a}_n, \hat{\tau}_n, \widehat{\boldsymbol{\theta}}_n^T, \widehat{\boldsymbol{\theta}}_n^R$. The result will include: 1) correctly estimated, 2) incorrectly estimated, 3) missing and 4) spurious rays. These can be directly compared to the original ideal ray parameters, $a_n, \tau_n, \boldsymbol{\theta}_n^T, \boldsymbol{\theta}_n^R$. Discrepancies between the ideal and distorted responses will be readily apparent. We use this approach here because it can potentially provide insights into the sources of error that yield incorrect ray estimates and possibly suggest strategies for mitigating them.

Alternatively, a larger set of simulations can be conducted and model parameters such as path loss, RMS delay spread, RMS angle spread, etc. for the distorted and ideal cases can be estimated and compared. This is likely more suitable during later stage work that focuses on the impact of errors in system model parameters on channel model parameter estimation.

D. Estimation of System Model Parameters

The performance of the cross-validation methodology is highly dependent upon the accuracy with which the parameters of the array system models can be estimated. The system impulse response and noise floor can be characterized by connecting the transmitter and receiver at the transmitting and receiving antenna connection planes, measuring the received signal and processing the response as described above. The result gives an accurate and complete indication of the temporal resolution of the channel sounder.

Obtaining the three-dimensional patterns of the transmitting and receiving antenna patterns of the antennas presents a greater challenge. Few vendors provide three-dimensional patterns of their products and considerable effort is required to measure them after they are purchased. For fixed antennas, the three-dimensional pattern can be approximated using the principal plane patterns but the impact on the results is not clear. Phased array antennas present a greater challenge because the antenna pattern changes with scan angle.

Determining the sensitivity of the cross-validation technique to uncertainty in the antenna pattern is an obvious next step. Ideally, this will allow us to set a minimum standard for acceptable antenna pattern accuracy.

III. RESULTS

Five of the research groups that are participating in the NIST-led 5G Millimeter-Wave Channel Model Alliance are using the cross-validation methodology to characterize and compare their 28 GHz channel sounders. In Sec. A, the characteristics of these channel sounders are summarized and demonstrate the variety of approaches and instrument configurations that are currently used. In Sec. B, some preliminary results are presented, including selected system response characterizations and comparison of ideal and distorted rays from the NIST channel sounder.

A. Description of the Channel Sounders

National Institute of Standards and Technology. The NIST 28 GHz channel sounder has an operating bandwidth of 1 GHz and provides 1-ns delay resolution [8]. The probing signal is a PN sequence (length 2^{15}) with direct sampling and off-line correlation performed at the receiver. The maximum measurable path loss is 165 dB and the dynamic range is 45 dB. The channel sweep time is 66 µs which allows characterization of mobile channels up to 140 km/h. The transmitting antenna is a 2 dBi dipole with omnidirectional coverage in azimuth and 90º beamwidth in elevation. The receiving antenna is a 16 × 1 switched-array system. Each array element is a 16.6 dBi gain horn with 45º beamwidth in both azimuth and elevation. The array FOV is 360º in azimuth and 90º beamwidth in elevation. The system can resolve AoA but not AoD.

University of British Columbia. The UBC 28 GHz channel sounder has an operating bandwidth of 1 GHz and provides 1 ns delay resolution [9]. The maximum measurable path loss is 165 dB and the dynamic range is 45 dB. The instrument is VNA-based with a nominal channel sweep time of 500 ms. In zero-span mode, the sampling time is 1 ms which permits characterization of fading on mobile channels up to 18 km/h. The transmitting antenna is an 18 dBi horn with 20º beamwidth in both planes. The receiving antenna is a dual-polarized 23 dBi horn with 13º beamwidth in both planes. Both antennas are mounted on identical azimuth-elevation positioners. The scan FOV is 360º in azimuth and +30º to -45º in elevation. The system can resolve both AoD and AoA.

University of Southern California. The USC 28-GHz channel sounder (jointly developed with researchers from Samsung) has an operating bandwidth of 400 MHz and provides 2.5 ns delay resolution [10]. The probing signal is a multi-carrier signal with modified Newman phases to minimize PAPR (Peak to Average Power Ratio). The maximum measurable path loss is 160 dB without averaging but can be increased up to 40 dB through averaging. Its dynamic range is > 100 dB. The channel sweep time is adjustable with values of 2-20 ms typical for dynamic channels. The transmitting and receiving antennas are both 8×2 phased arrays capable of resolving AoD and AoA, respectively. Each element has a gain of 5 dBi. The array presents 12º beamwidth in azimuth and 30º beamwidth in elevation over a FOV of 90º in azimuth and ±30º in elevation. The beam switching pattern, averaging, etc., are all configurable within an FPGA.

North Carolina State University. The NCSU 28 GHz channel sounder can be configured to operate with either a 1 GHz or 2 GHz operating bandwidth and provide delay resolutions of 1.33 ns and 0.67 ns, respectively [11]. The probing signal is based on a Zadoff-Chu sequence sampled at 3.07 GSa/s with 2× and 4× oversampling in the 2 GHz and 1 GHz modes, respectively. The maximum measurable path loss is 180 dB and the dynamic range is 60 dB. The channel sweep time is 1.33 µs without averaging. The transmitting and receiving antennas are both 17 dBi horns with 24º beamwidth in azimuth and 26º beamwidth in elevation. Both antennas are mounted on identical azimuth-elevation positioners. The scan FOV is 360º in azimuth and 120º in elevation. The system can resolve both AoD and AoA.

Technische Universität Ilmenau. The TU Ilmenau channel sounder can operate in either the 27-30 GHz or the 27-30 GHz frequency band. The maximum 10 dB bandwidth is 7 GHz which provides a delay resolution of 0.14 ns [12]. The probing signal is based on a Maximum-Length-Sequence with a length of either 12 or 15 bits. This provides an unambiguous range of 600 ns or 4.7 µs. The maximum measurable path loss is with the 16 dBi antennas at TX and RX 210 dB and under using of the 21 dBi antennas 220 dB. The system fully polarimetric works on TX with a switched polarization and at RX with dual polarization in parallel. The dynamic range depends on the number of averages and sequence length but is for the slow systems with 1024 hardware averages always greater than 60 dB. The fast system can record 13000 CIR/s without averaging and a dynamic range of around 45 dB. All directional antennas are mounted on azimuth-elevation positioners. The transmitting and receiving station can be pointed in discrete directions: in azimuth -180º to +180º in minimum 0.1º steps and in elevation to -75º to +75º in minimum 0.1º steps. The system can resolve both AoD and AoA. The full system has one transmitter station and two receiver stations, which makes it possible to handle two measuring points in parallel.

B. Model Parameters

The essential parameters of the array system model are: (a) the impulse response of the channel sounder observed with the transmitter connected directly to the receiver, (b) the patterns of the transmitting and receiving antennas, and (c) the thermal and (d) phase noise observed at the receiver. Each of the five participants characterized their systems in this manner. The corresponding measurements for the NIST channel sounder given in Fig. 3 are typical.

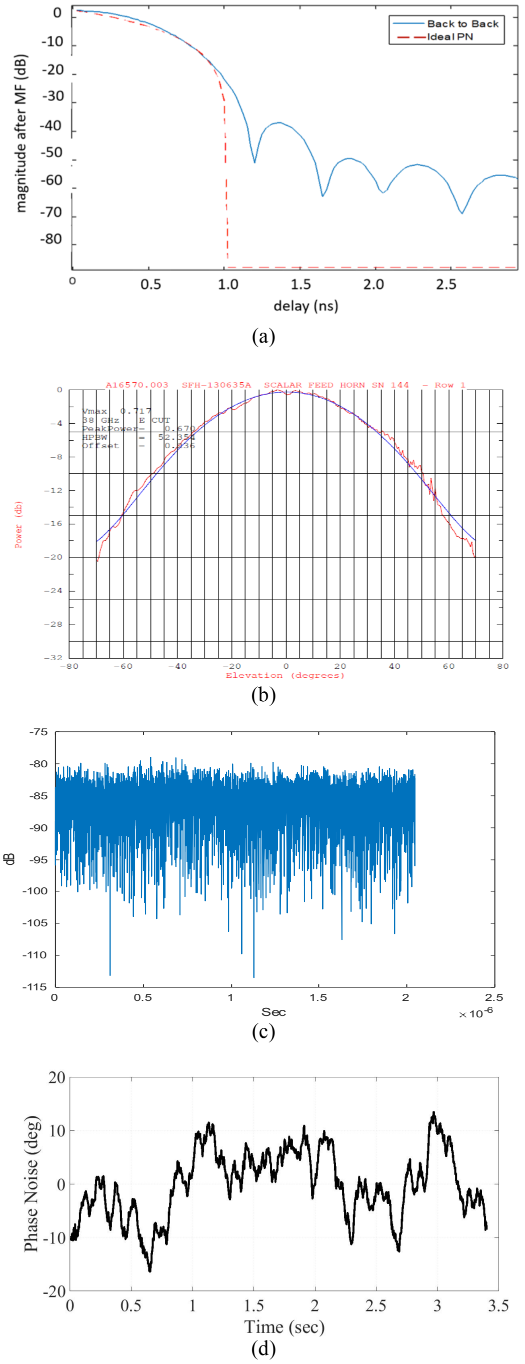

Fig. 3. Characteristics of the NIST channel sounder: (a) system impulse response, (b) transmitting and receiving antenna patterns, (c) thermal noise and (d) phase noise/drift.

C. Comparison of Simulated and Distorted MPCs

Missing and ghost MPCs observed with the NIST channel sounder, (a) after distortion of the ideal three-dimensional impulse response and (b) after MPC extraction using the SAGE algorithm, are depicted in Fig. 4 for NIST location 6. The bracketed numbers refer to individual power delay

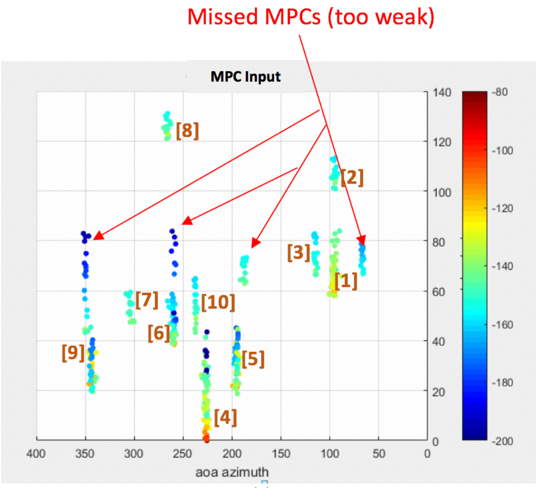

(a)

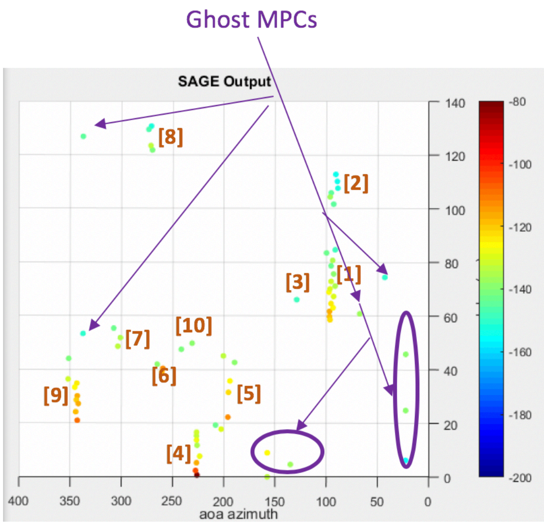

(b)

(c)

Fig. 4. Simulated missing and ghost MPCs observed with the NIST and TU-Ilmenau channel sounders: (a) after distortion of the ideal three-dimensional impulse response and (b) after MPC extraction using the SAGE algorithm. The horizontal axis is the angle of arrival in the azimuth plane in degrees and the vertical axis is the delay in ns.

profiles (PDPs) observed at particular AoAs. In Fig. 4(a), instances where simulated MPCs were missed because their responses fall below the noise threshold of the receiver are highlighted, *i.e.,* errors of omission. In Fig. 4(b), instances where the SAGE algorithm returned false or ghost MPCs, *i.e.,* errors of commission. In the next phase of this work, similar plots will be generated for the other channel sounders and their responses compared.

IV. Conclusions

To more easily compare performance of different channel sounders, we have developed an approach that involves degrading the ideal three-dimensional channel impulse response using distortion models that captures the factors that limit the spatio-temporal response of each channel sounder. In each case, discrepancies between the ideal and distorted three-dimensional channel impulse responses are readily visualized, and, importantly, the impact of the finite spatio-temporal resolution on the observed channel responses in a particular scenario assessed.

Implementation of the distortion model is straightforward. Measurement of the system impulse response and noise floor of the channel sounder are easily accomplished and yields a complete and accurate indication of the temporal resolution of the system. However, determination of the antenna patterns is more complicated as data provided by antenna manufacturers are usually not sufficiently accurate, so that a calibration of the specific array in an anechoic chamber or measurement range is required.

The next step will be to perform the same distortion and visualization methodology using the other four channel sounders and demonstrate the extent to which the performance of alternative channel sounders can be easily compared. Another task will be to determine the sensitivity of the results to uncertainty in the pattern and set a minimum acceptable standard for the measurement accuracy of the antenna pattern.

References

[1] L. M. Correia, *COST 259 - Wireless Personalized Mobile Communications*. Wiley, 2001.

[2] P. Almers et al., “Survey of channel and radio propagation models for wireless MIMO systems,” *EURASIP J. Wirel. Commun. Netw.*, vol. 2007, pp. 019070, 2007.

[3] K. Haneda, “Channel models and beamforming at millimetre-wave frequency bands, *IEICE Trans. Commun.*, vol. E98-B, no. 5, pp. 755-772, May 2015.

[4] B. H. Fleury *et al.*, “Channel parameter estimation in mobile radio environments using the SAGE algorithm,” *IEEE J. Sel. Areas Commun.*, vol. 17, no. 3, pp. 434–450, Mar. 1999.

[5] R. O. Schmidt, “Multiple emitter location and signal parameter estimation,” *IEEE Trans. Antennas Propag.*, vol. AP-34, no. 3, pp. 276–280, Mar. 1986.

[6] A. Richter, “Estimation of radio channel parameters: Models and algorithms,” Ph.D. dissertation, Dept. Elect. Eng. Inf. Technol., Technischen Univ. Ilmenau, Ilmenau, Germany, Dec. 2005.

[7] C. Lai, R. Sun, C. Gentile, “Methodology for Multipath-Component Tracking in Millimeter-Wave Channel Modeling,” In review, *IEEE Trans. Antennas Propag.*, 2018.

[8] P. B. Papazian, C. Gentile, K. A. Remley, *et al.* “A radio channel sounder for mobile millimeter-wave communications: System implementation and measurement assessment.” *IEEE Trans. Microw. Theory Tech.*, vol. 64, no. 9, pp. 2924-2932, 2016.

[9] B. N. Liya and D. G. Michelson, “Characterization of multipath persistence in device-to-device scenarios at 30 GHz,” in *Proc. Globecom Workshops* (Washington, DC), 2016, pp. 1-6.

[10] C. U. Bas *et al.,* “Real-time millimeter-wave MIMO channel sounder for dynamic directional measurements,” arXiv preprint arXiv:1807.11921, 2018.

[11] W. Khawaja *et al.*, “Effective of passive reflectors for enhancing coverage of 28 GHz mmWave systems in an outdoor setting,” in *Proc. IEEE RWS 2019*, pp. 1-5, 2019.

[12] R. Müller *et al.,* "Simultaneous multi-band channel sounding at mm-Wave frequencies," in *Proc. EuCAP* (Davos), 2016, pp. 1-5. doi: 10.1109/EuCAP.2016.7481757